PAPER ID: 0241
DOI: 10.18462/iir.compr.2017.0241

GEOMETRICAL ASPECTS OF NOVEL INTERNALLY GEARED SCREW MACHINE

Matthew Read, Nikola Stosic, Ian Smith

Centre for Compressor Technology

City, University of London

London, EC1V 0HB, UK, m.read@city.ac.uk

ABSTRACT

Cylindrical helical gearing can be used in a positive displacement machine where an externally lobed inner gear rotates inside an internally lobed outer gear while maintaining continuous lines of contact between the gears. This creates a series of separate working chambers between the rotors. In this type of machine the rotors have parallel axes of rotation, and both rotors can be free to rotate about their own axes. Fixed end plates are proposed as a method of controlling the period during which fluid is allowed to enter or leave the working chambers of the internally geared screw machine. As with conventional screw machines, these internally geared rotors can then be used to achieve compression or expansion of a trapped mass of fluid. This paper describes the geometrical analysis of some simple rotor profiles and explores the effect on rotor forces for particular applications of this novel screw configuration.

Keywords: Compressors, rotor profile, internal gearing, cycloid

1. INTRODUCTION

Conventional twin screw machines consist of two externally lobed helical rotors, which rotate about parallel axes within a fixed casing. The rotors are carefully shaped to ensure that lines of continuous contact occur between the rotors. This combined with the small clearance gap between the rotor tips and the casing creates a series of separate working chambers. The volume of a working chamber enclosed within the two rotors and the side and end faces of the casing is seen to vary with the angular position of the rotors. Carefully shaped holes, or ports, in the end faces of the casing then allow fluid to enter and leave the working chambers once specified volumes are reached, allowing either compression or expansion of the fluid passing through the machine.

Internally geared rotors are used in various configurations of pump, either as straight cut rotors (such as Gerotor or internal lobe pumps) or as helical rotors with open ends. An important feature of the rotor profiles is the requirement for continuous contact between rotors. Details of rotor profile generation for such applications are described by Colbourne (1974), Beard (1988), Beard et.al (1992), Vecchiato et.al (2001) and Litvin & Fuentes (2004). Moineau (1932) describes how the geometry of such rotors can be defined and proposes the use of rotors with variable pitch or variable profile in order to achieve a change in the volume of the working chamber between inlet and discharge of the machine. More recent developments have looked at implementing the concept of conical internally geared rotors for a range of compressor applications. There are considerable challenges in manufacturing rotors of this type with the requisite high accuracy using efficient and economical methods.

2. INTERNALLY GEARED SCREW MACHINES WITH PORTING

This paper focuses on characterising some important geometrical characteristics of a novel type of internally geared screw machine in which the rotors have constant pitch and profile. Both rotors are allowed to rotate about fixed parallel axes. An example of this arrangement is shown in Figure 1, and details of the required rotor geometry are discussion in the following section. With open ends, this configuration functions as a pump. The use of fixed end plates with porting however allows control over the periods during which fluid can enter and leave the working chamber, and the machine can therefore operate as either a compressor or expander. The shapes of the ports is discussed in more detail in section 2.3, and examples of ports at the high pressure end face of the rotors are shown in Figure 6. The constant pitch and profile of the helical rotors can potentially reduce the manufacturing complexity compared to the variable pitch and/or profile configuration; the inner rotor can be manufactured with high precision using the same methods as conventional twin screw rotors, while the outer rotors can potentially be made using internal grinding or additive manufacturing methods.

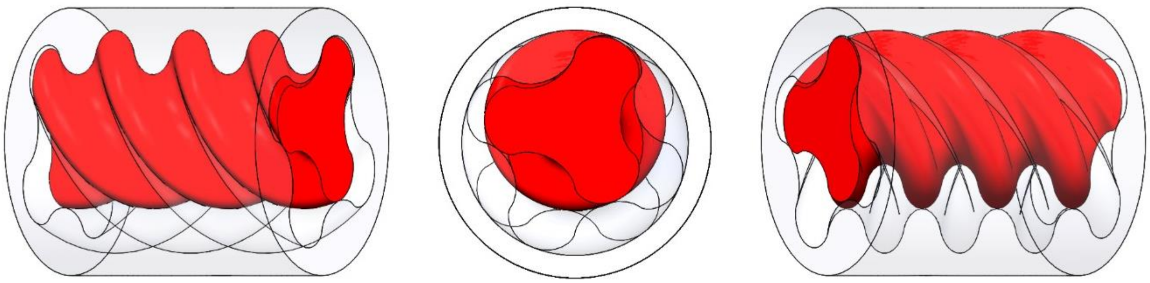

Figure 1: Views of an internally geared configuration with 3 lobes on inner rotor illustrating contact lines between the inner rotor (red) and the outer rotor (transparent) and the resulting working chambers

2.1. Internally Geared Rotor Profiles

Internally geared positive displacement machines require continuous contact points between inner and outer rotors during rotation about parallel axes. This allows the formation of enclosed working chambers whose volume varies with the angular position of the rotors. A wide range of rotor profiles can be generated that meet this requirement. In this paper, simple geometries consisting of epicycloids and hypocycloids are used to illustrate this requirement of continuous contact between rotors and to investigate machine performance. These profiles require that the inner rotor has one fewer lobe than the outer rotor. The equations defining coordinates of epicycloid and hypocycloid profiles are shown in Equations 1 and 2. While cycloids are used in this paper to illustrate the analysis of internally geared machines, it should be noted that there is considerable scope for optimisation using other methods of rotor profile generation.

$$\begin{bmatrix} x_e(\theta) \\ y_e(\theta) \end{bmatrix} = \begin{bmatrix} (\rho_b + \rho_e)\cos\theta - \rho_e \cos\big(\theta(\rho_b/\rho_e + 1)\big) \\ (\rho_b + \rho_e)\sin\theta - \rho_e \sin\big(\theta(\rho_b/\rho_e + 1)\big) \end{bmatrix} \qquad \text{Eq. (1)}$$

$$\begin{bmatrix} x_h(\theta) \\ y_h(\theta) \end{bmatrix} = \begin{bmatrix} (\rho_b - \rho_h)\cos\theta + \rho_h \cos\big(\theta(\rho_b/\rho_h - 1)\big) \\ (\rho_b - \rho_h)\sin\theta - \rho_h \sin\big(\theta(\rho_b/\rho_h - 1)\big) \end{bmatrix} \qquad \text{Eq. (2)}$$

Continuous contact between rotors can be achieved using composite profiles which can be created by combining sections of epicycloid and hypocycloid profiles. The profiles are defined by the radius of the base circle, ρ_b, the number of lobes required on the rotor, N, and the radius of the epicycloid generating circle, ρ_e, where $0 \leq \rho_e \leq \rho_b/N$. By considering the circumferences of the epicycloid and hypocycloid generating circles, it can be seen that the radius of the hypocycloid generating circle is:

$$\rho_h = \rho_b/N - \rho_e \qquad \text{Eq. (3)}$$

The maximum and minimum radii of the rotorcan easily be derived as follows, and it is clear that when $\rho_e = 0$ or $\rho_h = 0$, the rotor is a pure hypocycloid or epicycloid respectively.

$$\rho_{max} = \rho_b + 2\rho_e, \quad \rho_{min} = \rho_b(1 - 2/N) - 2\rho_e \qquad \text{Eq. (4)}$$

In order to achieve the required meshing condition between the inner and outer rotors it can be shown ρ_e and ρ_h must be equal for both rotors and that:

$$\rho_e/E = \rho_e/(\rho_e + \rho_h) \qquad \text{Eq. (5)}$$

It is clear from Equation 5 that the possible values of the ratio ρ_e/E range between zero and one, corresponding to the cases when the rotors are pure hypocycloids and epicycloids respectively. Examples of different rotor profiles are shown in Figure 2. In all the examples presented in this paper, the geometric parameters for the outer rotor have been chosen in order to achieve a maximum profile radius of 0.5 m, and the profiles are therefore bounded by a circle of diameter 1 m.

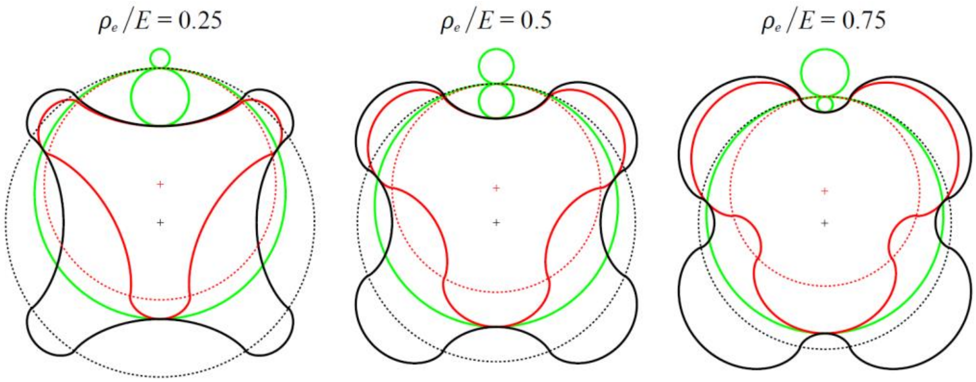

Figure 2: Inner (red) and outer (black) rotor profiles for values of $\rho_e/E = 0.25, 0.5$ and 0.75, showing loci of contact points during rotation (green) and rotor pitch circles (dotted lines)

2.2. Geometrical Characteristics of Internally Geared Screw Machines

Once the rotor profiles have been specified the contact points can be identified using the meshing condition for the two rotors. This states that the normal to the surface of both rotors at a point of contact must pass through the pitch point of the rotors, which is the point where the base circles of the inner and outer rotors coincide. The area contained between two rotor contact points can then be characterised as a function of the angular position of the rotor profiles. This working chamber area is seen to increase from zero (at the angular position where two contact points converge) to a maximum value, as shown in Figure 3. Due to the symmetry of the rotor lobes, the relationship of the working chamber area with the angular position is symmetrical about this point of maximum area.

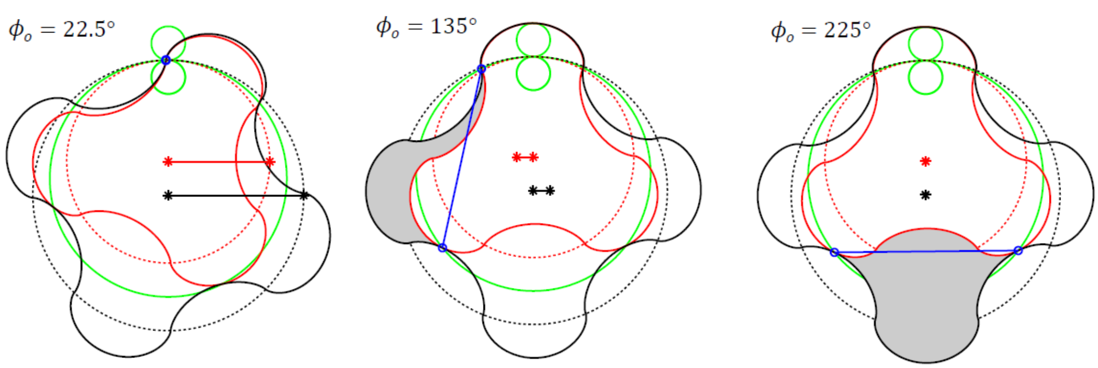

Figure 3: Cross-sectional area of working chamber at different angular positions of outer rotor, ϕ_o

For helical rotors at a fixed angular position, the variation of area with profile angular position can be related to the cross-sectional area of the working chamber as a function of longitudinal location. As for conventional screw machines, this requires the wrap angle of the rotors, $\phi_{w,o}$, to be defined along with the rotor length (Stosic et.al, 2005). The values used for the analysis presented in theis paper are specified in Table 1. Hence, for a specific rotor position, the volume of the working chamber can be found by performing an integration of the area w.r.t. the longitudinal coordinate, z. The working chamber volume can therefore be found as a function of rotor position as shown in Figure 4, and the swept volume per revolution of the outer rotor as a function of rotor profile is shown for a range of inner rotor lobe numbers.

Table 1: Characteristics of internal screw rotor geometry

Parameter	Value
Outer rotor length-diameter ratio, $L/2\rho_{o,max}$	1.55
Outer rotor wrap angle, $\phi_{w,o}$	300°

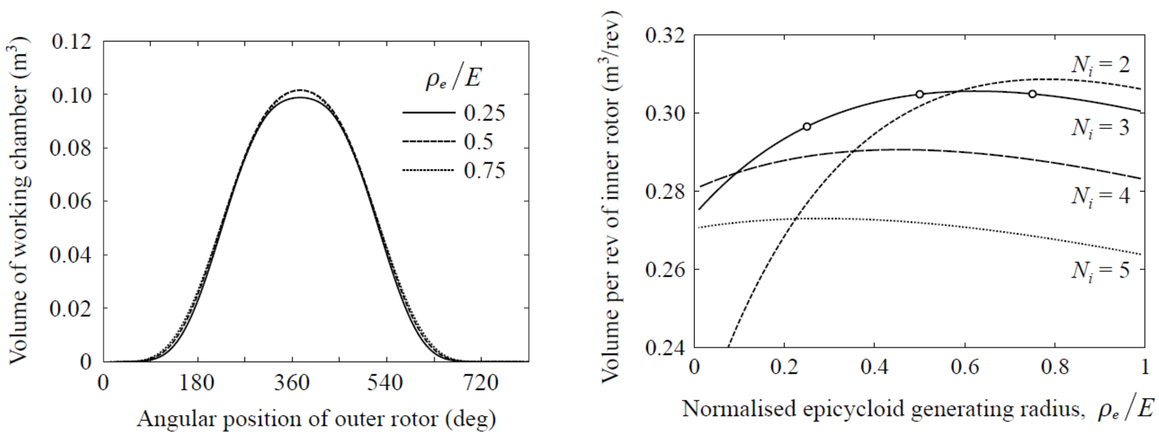

Figure 4: Volume of working chamber as a function of the rotor angular position, and a comparison of the effect of ρ_e/E and rotor lobe number on the swept volume of internally geared machines with simple epi/hypo cycloidal gear profiles

The results in Figure 4 suggest that for the simple composite cycloid profiles considered here, the value of ρ_e/E does not have a large effect on the swept volume for cases with $N_i > 2$. For $N_i = 3$ the difference between the maximum and minimum swept volume is seen to be less than 10%, and this decreases as N_i increases. Increasing N_i is seen to reduce the maximum possible swept volume, but the change is relatively small and there is clearly siginificant scope for optimising the overall performance of internally geared machines by varying both lobes number and profile.

Once the volume of the working chamber has been characterised as a function of rotor position, the performance of the machine can be investigated for particular applications. The key considerations in the analysis presented in this paper are the effect of geometry on the forces and torques that act on both the inner and outer rotors.

2.3. Performance Characteristics of Internally Geared Screw Machines

In order to investigate the operation of internally geared machines a number of assumptions have been made. The working fluid is assumed to be an ideal gas with $\gamma = 1.4$, and the compression process is assumed to be isentropic. The discharge pressure from the compressor is assumed to be equal to working chamber pressure after the compression process (i.e. there is no over or under compression), and the pressure is assumed to remain constant during filling and discharge of the working chamber. Leakage between the inner and outer rotors or between end plates and rotor end faces has also been neglected. These assumptions allow a simple investigation of the effects of rotor geometry, as radial forces and rotor torques can be derived from integration w.r.t. z (the longitudinal coordinate) of pressure acting on the projected area between rotor contact points. At a particular longitudinal position (i.e rotor cross-section), the contact points are used to find the projected length over which the pressure is acting, L_p. The resultant pressure force per unit length can be considered to act at the centre of this line and in a direction perpendicular to it. The torque arm distances, a_i and a_o, between the line of action of the pressure force and the rotational axes of the two rotors can then be found as shown in Figure 5. It is clear that the radial force on the two rotors must be of equal magnitude and opposite in direction. This force multiplied by the torque arm distances gives the rotor torques per unit length, which can then be integrated along the z coordinate to find the net torques.

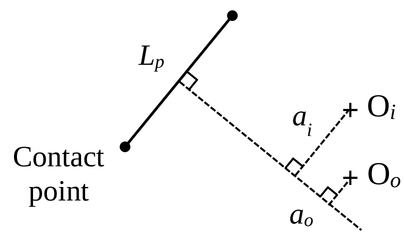

Figure 5 – Illustration of the geometry used to calculate radial force and rotor torques

Axial force can be found by calculating the pressure acting over the area of the working chamber surface on each rotor projected onto the end plane of the rotors. This requires the area bounded by the rotor profiles and the loci of contact points to be assessed for the working chamber in each rotor position, and the net axial force can be found by integrating the pressure multiplied by the projected area.

The built-in volume ratio (ε_v) of the machine is the ratio of the maximum working chamber volume to the minimum volume at which the working chamber remains closed from either the suction or discharge ports. The volume vs. rotor position curve allows the geometry of the suction and discharge ports to be defined in order to achieve a particular value of ε_v. This is achieved by identifying the position of the rotor profiles at the high pressure end face of the rotors at the point where the working chamber volume reaches the required value. These profiles are then used along with the loci of contact points to define a port area which ensures that flow can only enter or leave the working chamber once the required position is reached. Examples of the port shapes for some of the rotor geometries considered in this paper are shown in Figure 6.

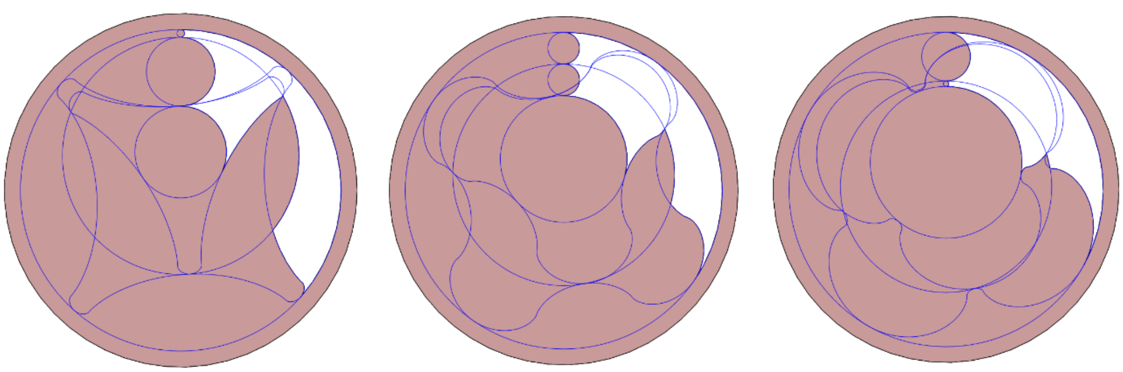

Figure 6: Examples of high pressure port geometry required to achieve $\varepsilon_v = 5$ with $\rho_e/E = 0.1, 0.5$ and 0.9 respectively using parameters in Table 1

Using $\varepsilon_v = 5$ as illustrated in Figure 6 and the assumptions described above, the net radial force, torque and axial force for three different rotor profiles have been calculated for applications with a constant suction pressure of 1 bar, and the results are shown in Figures 7-9.

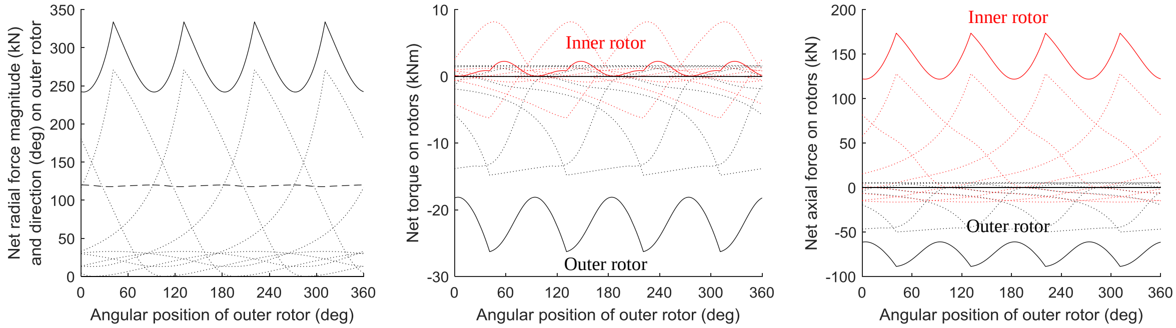

Figure 7: Net radial force, torque and axial force on rotors with $\rho_e/E = 0.9$, $p_{suc} = 1\ bar$, $\varepsilon_v = 5$ (results from individual working chambers are shown as dotted lines, while the net results are shown as solid lines; red for inner and black for outer rotors)

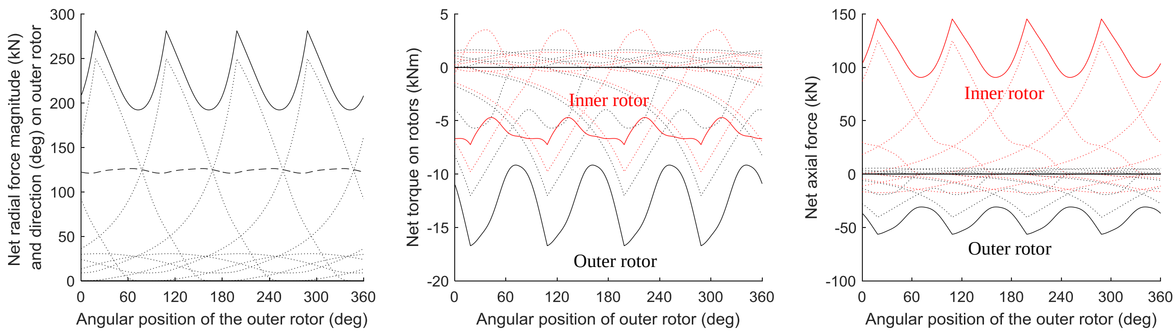

Figure 8: Net radial force, torque and axial force on rotors with $\rho_e/E = 0.5$, $p_{suc} = 1\ bar$, $\varepsilon_v = 5$ (results from individual working chambers are shown as dotted lines, while the net results are shown as solid lines; red for inner and black for outer rotors)

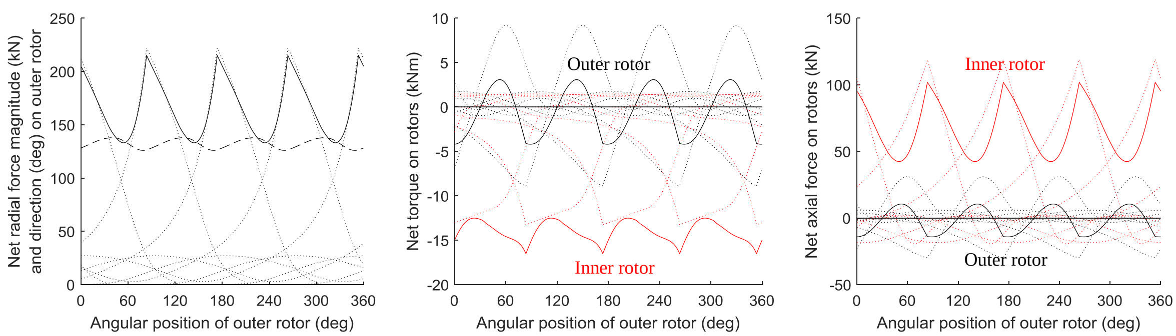

Figure 9: Net radial force, torque and axial force on rotors with $\rho_e/E = 0.1$, $p_{suc} = 1\ bar$, $\varepsilon_v = 5$ (results from individual working chambers are shown as dotted lines, while the net results are shown as solid lines; red for inner and black for outer rotors)

It is possible to check the net torque for these profiles by calculating the work done per revolution of the outer rotor for the isentropic process with the average torques of the two rotors, as shown in Equations 6 and 7:

$$W_{cyc} = \left(\frac{\gamma}{\gamma-1}\right)\left(P_{dis}(V_{max}/\varepsilon_v) - P_{suc}V_{max}\right) \quad \text{Eq. (6)}$$

$$P = W_{cyc}N_o\frac{\omega_o}{2\pi} = \omega_o\left(\bar{T}_o + \bar{T}_i(N_o/N_i)\right) \quad \text{Eq. (7)}$$

where $\bar{T}$ is the time averaged value of the rotor torque. In all cases presented here, the torque values calculated using the numerical integration described are found to agree with the calculated work done to within 0.1%.

The three examples shown in Figures 7-9 illustrate the importance of rotor profile on the operation of the internally geared machine. It is clear that for a compressor, the rotor with the largest time averaged torque should be the driven rotor as this will mean that more of the shaft power driving the compressor is delivered directly to the fluid, and the contact force between the rotors will be reduced. When $\rho_e/E = 0.9$ (Figure 7) it is clear that the ratio of inner/outer rotor torque is very low. This is advantageous as it means that if the outer rotor is driven there will be very low contact force between the rotors. This torque ratio increases for $\rho_e/E = 0.5$ and the stress at the contact points is therefore significantly higher. For $\rho_e/E = 0.1$ the inner rotor now has the higher torque, with the outer rotor torque varying between positive and negative. If the inner rotor is now driven then the contact force will be reduced, but the oscillating torque on the outer rotor will still cause significant maximum contact forces due to the driven/undriven torque ratio varying from around 0.3 to -0.2. It can also be seen in Figures 7-9 that as ρ_e/E decreases the magnitude of the mean axial and radial forces acting on both rotors also decrease.

3. CONCLUSIONS

The analysis presented in this paper illustrates the characteristics of a novel internally geared positive displacement machine. The key principle of constant pitch and profile rotors rotating about fixed, parallel axes has ben described. Examples of simple cycloidal rotor profiles that meet the requirement of continuous contact between rotors have been decribed. The concept of stationary end face porting required to achieve compression or expansion of fluid in such a device has been discussed and examples of the high pressure ports presented. The simple model of an ideal compression process has been used to investigate the forces exerted on the rotors, leading to the following conclusions.

- For the simple composite cycloidal profiles, the time averaged torque on the inner or outer rotor can be minimized by selection of the value of ρ_e/E.
- In the examples presented, the average inner rotor torque is minimised with $\rho_e/E \approx 0.9$, while the average outer rotor torque is minimised with a $\rho_e/E \approx 0.1$.
- The results show that the ratio of undriven to driven rotor torques remains closer to zero in the case with $\rho_e/E = 0.9$. However, the axial and radial forces are seen to decrease with decreasing values of ρ_e/E, and this case will therefore have larger bearing loads than those with lower ρ_e/E. The swept volume for this case is also 5% lower than the maximum, which occurs when $\rho_e/E \approx 0.5$.

The results show that there is significant scope to optimise the rotor geometry depending on the application. Future work will focus on developing a more detailed understanding of the machine performance. This will include characterisation of sealing line lengths and leakage flows, port areas as a function of working chamber volume, and alternative rotor profiles.

NOMENCLATURE

p	pressure (bar)	E	distance between rotor axes (m)
L	length (m)	N	number of lobes on rotor
V	volume (m^3)	P	power (W)
T	torque (Nm)	W_{cvc}	work done per cycle (J)
ρ	diameter (m)	ω	angular speed (rad/s)
ϕ	angular position of rotor (rad)	θ	cycloid generating angle (rad)
ϕ_w	wrap angle of rotor (rad)	ε_v	built-in volume ratio

REFERENCES

Moineau, R.J.L., 1932. *Gear mechanism*. U.S. Patent 1,892,217.

Colbourne, J.R., 1974. The geometry of trochoid envelopes and their application in rotary pumps. Mechanism and Machine Theory, 9(3-4), pp.421-435.

Beard, J.E., 1985. Kinematic analysis of gerotor type pumps, engines, and compressors, PhD thesis.

Beard, J.E., Yannitell, D.W. and Pennock, G.R., 1992. The effects of the generating pin size and placement on the curvature and displacement of epitrochoidal gerotors. Mechanism and Machine Theory, 27(4), pp.373-389.

Vecchiato, D., Demenego, A., Argyris, J. and Litvin, F.L., 2001. Geometry of a cycloidal pump. Computer methods in applied mechanics and engineering, 190(18), pp.2309-2330.

Litvin, F.L. and Fuentes, A., 2004. Gear geometry and applied theory. Cambridge University Press.

Stosic, N., Smith, I. and Kovacevic, A., 2005. Screw compressors: mathematical modelling and performance calculation. Springer Science & Business Media.